



Università degli Studi di Bari Aldo Moro

Dipartimento Interateneo di Fisica

Dottorato In Fisica XXXI Ciclo

Search for resonances in lepton decay with CMS at LHC

Relazione di fine Secondo Anno

Tutor:
Dott.ssa Anna Colaleo

Dottorando:
Filippo Errico

Chapter 1

Search for resonances decaying into two muons

My PhD activity deals with the search for resonances decaying into two muons with the CMS detector [1] at CERN. CMS has a dedicated system to detect muons (the so called muons system) composed of different detectors (DT, RPC and CSC — currently also GEM) which allows to measure muon momentum with a resolution less than 20% for high- p_T muons (~ 2 TeV) [2].

In particular I am focusing on the search of a low mass resonance, the Standard Model Higgs, and a massive resonance (with a mass of the order of TeV), the Z' boson.

1.1 Standard Model Higgs

I am involved in the search of Standard Model Higgs decaying into two muons.

At the LHC four SM fermions can have their couplings to the Higgs boson (H) measured: the top quark (t), bottom quark (b), the tau lepton (τ), and the muon (μ). Combined measurements from CMS and ATLAS of the 7 and 8 TeV proton-proton collision data have constrained the $H \rightarrow \tau^+\tau^-$ and $H \rightarrow b\bar{b}$ decay rates to be within 35% and 60% of their SM values, respectively, with 68% confidence [3].

This $\mu\mu$ channel instead still misses: it has, for a 125 GeV Higgs boson, a branching fraction of 0.02 %, much smaller than $b\bar{b}$ (58.2 %) and $\tau^+\tau^-$ (6.3 %) [7]. Nevertheless, due to the Higgs natural width (~ 4 MeV) and excellent muon momentum resolution at CMS, most $H \rightarrow \mu\mu$ events can be measured with an invariant dimuon mass resolution of 1.5 to 2.5 GeV. This enables us to discriminate the expected signal events against the vast quantities of high-mass, off-shell $Z \rightarrow \mu^+\mu^-$ decays, as well as leptonic $t\bar{t}$ decays, which form the main backgrounds.

The $H \rightarrow \mu\mu$ cross section measurement will provide three unique probes of SM Higgs boson properties [4]:

- it is the only way to directly measure the Higgs-muon Yukawa coupling strength,

and compare it to the muon mass

- the ratio of the $H \rightarrow \mu\mu$ to $H \rightarrow \tau\tau$ cross sections will provide constraints on the proportionality of the Higgs couplings to fermions of different generations, and of leptons with different masses
- the $H \rightarrow \mu\mu$ cross section will be of crucial importance if the hints of lepton flavor-violating $H \rightarrow \tau\mu$ decays seen at CMS become more significant.

The best results to date on Higgs coupling to second fermion generation, with 2016 data, are: $2.64 \times \text{SM}$ for 13 TeV for the observed limit on the rate of production of a Higgs boson with the mass of $125 \text{ GeV}/c^2$ and 0.9 ± 0.9 for the signal strength of σ/σ_{SM} . In order to improve these results, obtained with cut flow selection, this analysis will be performed with the multivariate analysis approach: the idea is to create a variable, starting from the usual ones (e.g. mass, momentum), in order to be able to separate signal and background as much as possible; this distribution will be used for limit extraction. In Figure 1.1 and 1.2, an example of a variable obtained with a neutral network and decision tree.

I am starting to analyze 2016 data, corresponding to 35.9 fb^{-1} in order to be ready for winter conferences.

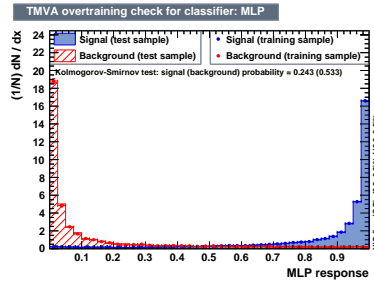


Figure 1.1: Multivariate analysis: MLP output score (training and test).

Next step: Set the analysis framework for 2016 data before to analyze data collected during the entire 2017.

1.2 Z' analysis

The current Particle Physics is well described by the Standard Model (SM) even if there are some aspects SM is not able to take into account (e.g. dark matter, gravitational force). In order to try to solve these issues, many models have been developed beyond Standard Model (BSM) and within these new bosons, like Z' , are introduced: examples include models described with extended gauge groups, featuring additional U(1) symmetries such as the Sequential Standard Model (SSM) [5] that includes a Z'_{SSM} boson with SM-like couplings, the Grand Unification Theories (GUT) inspired SSM models,

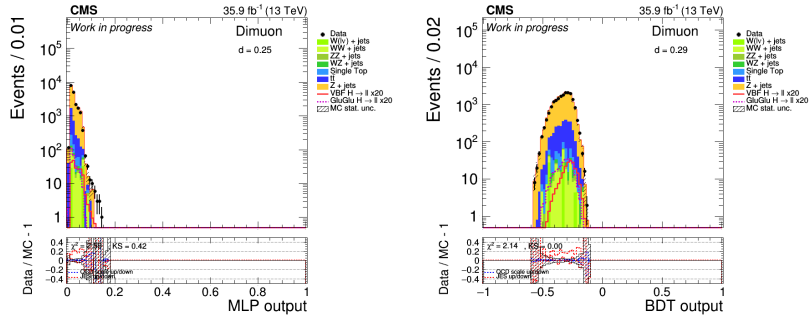


Figure 1.2: Multivariate analysis: validation of MLP (left) and BDT (right) input variables.

based on E6 gauge group, with a Z'_ψ boson and the Kaluza - Klein graviton (GKK) of the Randall - Sundrum (RS) model of the Extra Dimensions [6].

1.2.1 Mass distribution

I was focusing on the search of Z' boson decaying into two muons: this channel benefits from high signal selection efficiencies and relatively small, well-understood, backgrounds. The dominant and irreducible SM background arises from Drell-Yan (DY) production (Z/γ^*) of e^+e^- and $\mu^+\mu^-$ pairs. Additional sources of background are top - antitop quark ($t\bar{t}$) and single top quark (tW), Drell-Yan $\tau^+\tau^-$ and diboson (WW, ZZ, WZ), in which the two prompt leptons are from different particles. These processes are estimated using Monte Carlo (MC) simulated events at the next-to-leading order (NLO) and corrected to the next-to-next-to-leading order (NNLO). Events in which at least one lepton candidate is a misidentified jet (W+jets, γ +jets and multijets) contribute a small background in the mass region of interest. These contributions are estimated from data.

I have analyzed 2016 data, corresponding to 36.3 fb^{-1} ; in Figure 1.3, the comparison between data and Monte Carlo of the dilepton mass distribution is shown without evidence for a signal deviation from the SM expectations.

In order to handle properly the different muon momentum resolution between barrel and endcaps, the scale bias and any source of inefficiency, the analysis is performed in two pseudorapidity categories: barrel-barrel (BB) events in which both muons are in the barrel and events with at least one of the two muons in the endcaps (BE). The corresponding mass distributions are shown in Figure 1.4

1.2.2 Mass scale

The response of the detector to the dilepton mass may evolve as the mass increases: as the muon p_T increases, it becomes more and more sensitive to the detector alignment. To estimate the effect of the p_T bias to the dimuon mass, I have recomputed the Drell-Yan

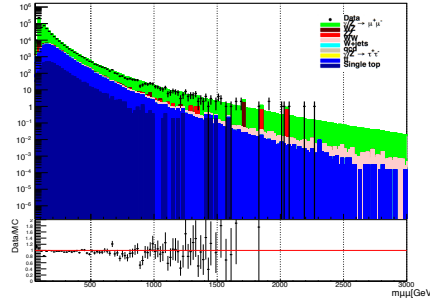


Figure 1.3: The invariant mass spectrum, together with the predicted SM backgrounds, for the $\mu\mu$ channel. No evidence for a signal deviation from the SM expectations is observed.

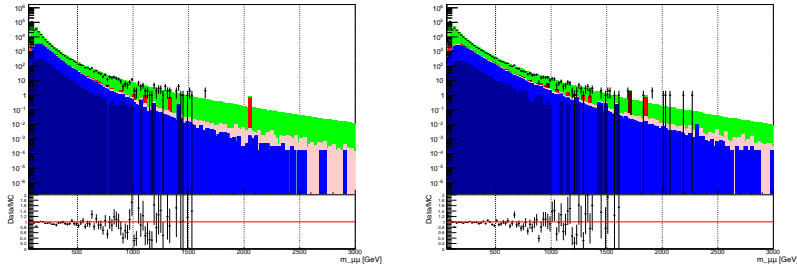


Figure 1.4: The invariant mass spectrum, together with the predicted SM backgrounds, for the $\mu\mu$ channel: on the left in BB category and on the right in BE. No evidence for a signal deviation from the SM expectations is observed.

mass in simulation by applying a shift to the muon p_T . The shift is applied to each muon and as a function of η and ϕ . For each muon the shift is done according to a Gaussian that takes as central value the central correction and as width the error assigned on the measurement. This correction has been performed only for the BE+EE category, given the p_T bias consistent with zero in the barrel. Figure 1.5 shows the difference between the invariant masses resolutions obtained with the p_T corrected by the p_T bias and the nominal one for the BE category. The observed difference is within 20 %.

On the other hand, with the aim to estimate the effect of the measured p_T bias also to the dimuon mass reconstructed on data, I have recomputed the mass by applying a shift to the muon p_T . To correct data, a shift is applied to each muon as a function of η and ϕ (using the same value as before); no gaussian smearing is considered. This correction has been performed only for the BE events. For different mass ranges, the relative residuals have been plotted comparing the reconstructed mass with the value obtained correcting the muon p_T in data: $((\text{mass} - \text{mass}_{\text{corrected}})/\text{mass})$. Figure 1.6 shows the mean value

of such distributions as a function of the mass. No shift is observed in the mass value correcting by the p_T bias. The maximum shift observed is within 0.2% up to 800 GeV and within 1% at higher masses.

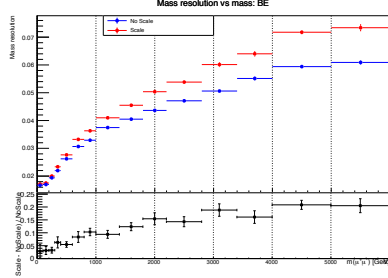


Figure 1.5: Observed difference between mass resolution as a function of the mass with and without the p_T scale propagated, for DY simulated events.

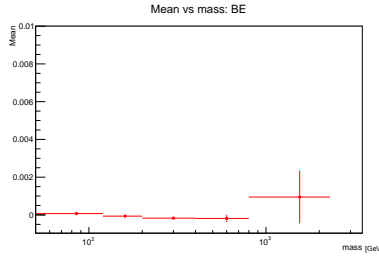


Figure 1.6: Mean value, as a function of the mass, of the relative mass residuals estimated comparing the reconstructed mass with and without the p_T bias correction in data.

1.2.3 MC distribution mass fit

In order to test for the existence of a resonance, a shape analysis has been performed using an unbinned maximum likelihood fit of dimuon invariant mass values m (the observable) to search for a resonant peak on-top of the smooth background distribution. Data is fit with a sum of signal and background shapes: while signal has been parametrized by the convolution of a Breit-Wigner (describing the intrinsic signal shape) and a Gaussian distribution (describing the experimental resolution), background parametrization has been obtained by fitting the SM simulated background distribution. I have fit the distribution mass in order to obtain the probability density function used to extract limit; the distribution has been fit combining two different function in the mass range [150,

6000] GeV:

$$f_{bkg}(m|a_{L,H}, b_{L,H}, c_{L,H}, d, k_{L,H}) = \begin{cases} e^{a_L+b_L \times m+c_L \times m^2} \times m^{k_L}, & \text{if } m < 500 \text{ GeV} \\ e^{a_H+b_H \times m+c_H \times m^2+d \times m^3} \times m^{k_H}, & \text{if } m > 500 \text{ GeV} \end{cases} \quad (1.1)$$

Split the function allow a better fit of the distribution, specially in the tail.

In Figure 1.7, the fit of the MC mass distributions are shown for Barrel - Barrel and Barrel - Endcap & Endcap - Endcap Region.

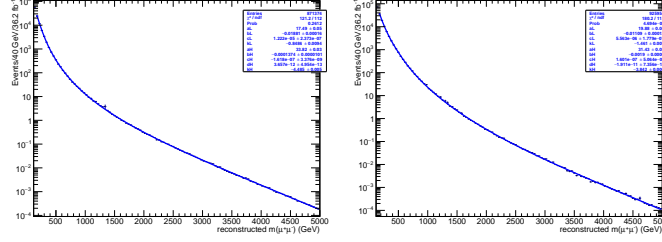


Figure 1.7: Fit of the simulated mass distribution: on the left for BB category; on the right for BE.

The final limit, set on the parameter R_σ which is the ratio of the cross section for dilepton production through a Z' boson to the cross section for dilepton production through a Z boson, are shown in Figure 1.8.

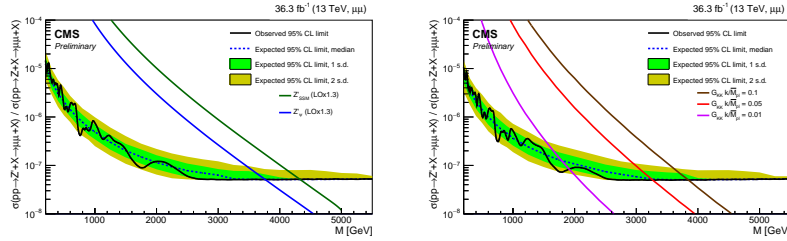


Figure 1.8: Final limits: on the left for Spin 1 resonance; on the right for Spin 2.

For the Z'_{SSM} particle and for the superstring inspired Z'_ψ particle, 95% confidence level lower mass limits are found to be 4.3 TeV and 3.75 TeV. The corresponding limits for Kaluza-Klein gravitons (G_{KK}) arising in the Randall - Sundrum model of extra dimensions depends on k/M_{pl} and ranges from 1.9 TeV to 3.85 TeV.

1.2.4 2017 Data

At the end of October, CMS has been able to collect 40.21 fb^{-1} for 2017 RunII. I have started to have a look at the first certified 18.7 fb^{-1} for muon studies. In Figure 1.9, the distribution mass for 2017 data compared with 2016 Monte Carlo simulations (2017

MC production is ongoing).

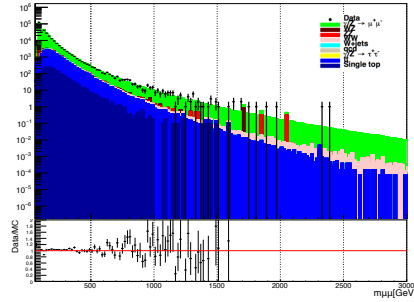


Figure 1.9: The invariant mass spectrum, together with the predicted SM backgrounds, for the $\mu\mu$ channel.

Next step: Analyse 2017 Data for Z' search, focusing on the study of the systematic.

Chapter 2

School & conferences

2.1 School

- CMSPhysics Object School, 4 - 8 September, Bari. (as facilitator)
<https://indico.cern.ch/event/615859/>
- INFN School of Statistics 2017; 7 -11 May, Ischia.
<https://agenda.infn.it/conferenceDisplay.py?confId=12288>

2.2 Conferences

- EPS-HEP2017: EPS Conference on High Energy Physics, 5-12 Jul 2017, Venice (Italy)
<http://eps-hep2017.eu>
- IFAE2017: XVI Incontri di fisica delle alte energie, 19-21 Apr 2017, Trieste (Italy)
<https://agenda.infn.it/conferenceDisplay.py?confId=12289>
- Posters@LHCC: Students' Poster Session at the 2017 Winter LHCC meeting, 22 Feb 2017, CERN, Geneva (Switzerland)
<https://indico.cern.ch/event/608530/>

Bibliography

- [1] CMS Collaboration, "The CMS experiment at the CERN LHC", JINST 3:S08004,2008
- [2] CMS Collaboration, "Performance of muon reconstruction including Alignment Position Errors for 2016 Collision Data", CMS DP-2016/067
- [3] ATLAS, CMS Collaboration, "Measurements of the Higgs boson production and decay rates and constraints on its couplings from a combined ATLAS and CMS analysis of the LHC pp collision data at $\sqrt{s} = 7$ and 8 TeV", JHEP 08 (2016) 045, doi:10.1007/JHEP08(2016)045, arXiv:1606.02266.
- [4] CMS Collaboration, "Search for Lepton-Flavour-Violating Decays of the Higgs Boson", Phys. Lett. B749 (2015) 337-362, doi:10.1016/j.physletb.2015.07.053, arXiv:1502.07400.
- [5] A. Leike, "The Phenomenology of Extra Neutral Gauge Bosons", Phys. Rept. 317 (1999) 143, [hep-ph/9805494]
- [6] L. Randall, R. Sundrum, "A Large Mass Hierarchy from a Small Extra Dimension", Phys. Rev. Lett. 83 (1999) 3370, [hep-ph/9905221]
- [7] LHC Higgs Cross Section Working Group et al, "Handbook of LHC Higgs Cross Sections: 3. Higgs Properties", CERN-2013-004 (CERN, Geneva, 2013) doi:10.5170/CERN-2013-004, arXiv:1307.1347